1

Chemical Vapour Deposition of CNTs Using Structural Nanoparticle Catalysts

G. N. Ayre, T. Uchino, B. Mazumder, A. L. Hector,
D. C. Smith, P. Ashburn and C. H. de Groot
University of Southampton
United Kingdom

J. L. Hutchison
Oxford University
United Kingdom

1. Introduction

The extraordinary mechanical, electrical and optical properties of CNTs have stimulated extensive research since their discovery by Sumio Iijima of the NEC Corporation in the early 1990s (Iijima, 1991). Possible applications for carbon nanotubes range from nanoelectronics, quantum wire interconnects, sensors and field emitters to composites (Meyyappan et al., 2005). These applications require reliable synthesis techniques capable of generating large quantities of high purity material. In addition, applications in nanoelectronics and photonics may require controlled growth at precise lithographically patterned areas. Understanding how to control the synthesis of SWNTs is vital in order to deterministically integrate such nanostructures into various technologies.

Of the various methodologies developed for carbon nanotube (CNT) synthesis, those based upon catalyst-assisted chemical vapour deposition (CCVD) appear to be best suited to satisfy these requirements. Traditionally, 3*d* valence transition metal nanoparticles, such as Fe, Co and Ni, are used to catalyse CNT growth. These catalysts are thought to work in accordance with the model for carbon filament growth, derived by Baker et al. (Baker, 1989; Baker et al., 1972; 1973), from concepts of vapour-solid-liquid theory (Wagner & Ellis, 1964). In this model, hydrocarbons adsorbed on the metal nanoparticle are catalytically decomposed resulting in atomic carbon dissolving into the liquid catalyst particle, and when a supersaturated state is reached, carbon precipitates in a tubular, crystalline form.

Recently, several groups have reported successful growth of CNTs from noble metal (Lee et al., 2005; Takagi et al., 2006; Yoshihara et al., 2008; Yuan et al., 2008; Zhou et al., 2006), ceramic (Liu et al., 2008b; Steiner et al., 2009) and semiconducting nanoparticles (Takagi et al., 2007; Uchino et al., 2009; 2008; 2005b), all of which are regarded as unable to catalyse the dissociation of hydrocarbons. In addition to this, in their bulk form, these materials do not have a catalytic function to produce graphite. This implies that given enough energy, carbon atoms on a nanoparticle are capable of a structural reorganisation into CNTs. This leads to a new in-

terpretation of the role of the catalyst in nanotube growth in which only a nanoscale curvature and carbon adsorption sites are necessary.
This work examines the recent developments in non-traditional CCVD of CNTs with a view to determine the essential role of the catalyst in nanotube growth. Section 2 provides a brief overview of the techniques reliant on the structural reorganization of carbon to form CNTs. An in-depth analysis of CNT synthesis based upon ceramic (Section 3), noble metal (Section 4) and semiconducting nanoparticle catalysts (Section 5) is presented. Various approaches to germanium catalyst preparation are compared in terms of growth density and quality of synthesized nanotubes. Scanning electron microscopy measurements indicate that a technologically relevant density is achievable using non conventional catalysts. Raman measurements have identified the synthesized nanotubes as single walled and, in terms of graphitization and structure, of a high quality. Extensive atomic force microscopy characterisation of the catalyst has been undertaken in order to ascertain the influence of morphology on the ability of the catalyst to yield CNT growth. A model for CNT growth consistent with the experimental results is proposed in Section 6. Finally, a summary of challenges and future directions for investigations is presented in Section 7.

2. Catalyst Free Synthesis of CNTs

Silicon carbide has been the most widely used non metallic catalyst. The synthesis techniques involving this catalyst have produced high densities of carbon nanostructures by annealing either SiC particles (Botti et al., 2004; Takikawa et al., 1998), amorphous SiC films (Botti et al., 2001; Kusonoki et al., 1997) or hexagonal SiC (6H-SiC) (Derycke et al., 2002; Kusonoki et al., 1997) in a vacuum. In these methodologies, the nanotube formation can be explained by the mechanism proposed by Kusonoki et al. (1997). Owing to the low vacuum in the chamber when annealing, the SiC oxidises forming SiO_2. As a consequence, the carbon atoms are free to bond with other atoms. If they bond to neighbouring carbon atoms, graphite fragments are formed containing dangling bonds. Thermodynamics drives the folding of graphitic fragments so that the dangling bonds of opposite edges are saturated. The as-formed nanotube segments act as seeds for the attachment of new carbon atoms, leading to CNT growth. However, these techniques require high temperature annealing at approximately 1650 $^{\circ}$C.
An alternate approach involves using carbon nanoparticles as a catalyst. This technique depends on the structural reorganization of carbon aggregates into nanotubes upon annealing. Botti et al. (2002) report a dense array of CNTs grown on silicon by spraying amorphous hydrogenated carbon nanoparticles on a Si substrate. Other similar approaches have been reported in the literature (Koshio et al., 2002; Larciprete et al., 2002; 2003).
Figure 1 shows transmission electron microscope images of carbon nanostructures deposited on a carbon implanted Ge nanoparticle sample. By inspection of Figure 1(a) it can be determined that this is made up of a collection of small multi-walled carbon nanotubes (MWNTs). As there were no catalyst particles detected at either ends of the nanotubes, it is therefore believed that these nanotubes were nucleated by the structural reorganization of amorphous carbon deposits without the influence of the Ge nanoparticles. This hypothesis is further reinforced by Figure 1(b), which shows a double walled nanotube (DWNT) in the early stages of growth. Again, there is no catalyst detected, and it appears that the nanotube was nucleated from the nearby carbon deposits. Both nanostructures demonstrate a good degree of graphitization and furthermore there are few impurities present, such as amorphous carbon, in the materials.

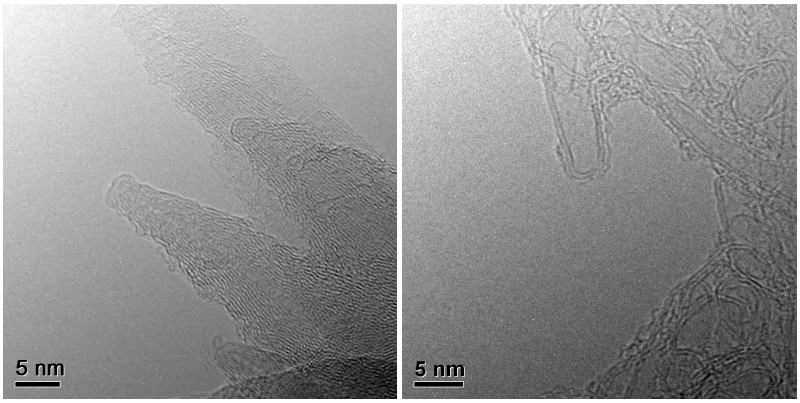

(a) (b)

Fig. 1. Transmission electron micrographs of self-assembled carbon nanostructures deposited on a carbon implanted Ge nanoparticle sample. The TEM sample was prepared by scraping the substrate surface with a surgical blade and collecting the material on a holey-carbon TEM grid. (a) Image of MWNTs and (b) a DWNT in the early stages of growth formed by the structural reorganization of carbon.

These techniques, although not strictly classed as chemical vapour deposition of CNTs, provide some insight into the behaviour of carbon aggregates at elevated temperatures without the influence of an external catalyst with a function to produce graphite. These results also demonstrate that regardless of the catalyst, the formation of CNTs involves two important processes: (i) the diffusion of carbon and (ii) the nucleation of a graphitic cap or fragment followed by the further incorporation of carbon into the growing nanotube. It has been reported that the diffusion process on a nanoparticle surface or across its interior is a rate limiting step (Bartsch et al., 2005; Hofmann et al., 2005), while the chirality of the growing CNT is decided upon the formation of the graphitic cap (Reich et al., 2006; Yazyev & Pasquarello, 2008).

3. Ceramic Nanoparticle Catalysts

Ceramic materials, such as Al_2O_3, have typically been used as a buffer layer to disperse metallic catalyst particles and enhance their catalytic properties in CNT growth (Takagi et al., 2007). However, the simplistic view that the support only plays a catalytically passive role in the formation of carbon nanotubes requires some examination. Rummeli et al. (2007) demonstrated that under typical conditions for CVD growth of CNTs, nanoparticles of difficult-to-reduce metal-oxides are exceedingly good at promoting ordered carbon (graphene) growth. As was expected, there was no observation of ordered carbon formation in bulk/film samples. This difference was attributed to the presence of surface defect sites on the nanoparticle oxides, and it was argued that in the substrate-based CNT synthesis routes, the interface between the catalyst particle and the surface behaves as an annular defect site. These sites would then promote the formation of cylindrical graphene structures, or nanotubes.

A recent study by Liu et al. (2008b) reports the formation of dense CNT layers catalysed by Al_2O_3 nanoparticles. Raman spectra of the synthesized nanotubes indicated that the nan-

otubes synthesized were predominantly single walled and of a good quality. Interestingly, the authors surmise that the mechanism of formation is different from the traditional vapour-liquid-solid mechanism as the nanoparticles are likely to be in the solid state during growth. This finding reinforces the argument of Rummeli et al. (2007), and additionally indicates that the growth of single-walled carbon nanotubes (SWNTs) on flat Al_2O_3 substrates may be possible by nanostructuring their surfaces. This hypothesis was partially confirmed by Liu et al. (2009) using a nanostructured SiO_2 substrate to grow SWNTs.
Another ceramic catalyst reported in the literature is ZrO_2 (Steiner et al., 2009). In this publication, dense growth of either MWNTs or SWNTs was possible, depending on the carbon feedstock used. ZrO_2 was typically deposited on either Al_2O_3 capped SiO_2 supports or Si substrates with an oxynitride support through a chloride salt solution. Samples were pretreated in H_2 prior to the introduction of the carbon feedstock. ZrO_2 is known to not be reduced by H_2 (Mctaggart, 1961) and additionally, carbothermic reduction of ZrO_2 does not yield Zr metal, but results in the formation of ZrC (Berger et al., 1999). In-situ x-ray photoelectron spectroscopy (XPS) revealed that the state of the catalyst after H_2 pretreatment showed two phases; a stoichiometric and an oxygen deficient phase of zirconia. The role of the H_2 pretreatment in this work, while shown not to result in the formation of Zr metal, is thought to introduce surface defect sites into zirconia nanoparticles that aid in enhancing catalytic ability. It should be noted that, as observed by in-situ XPS, CNT growth seems to begin only after the introduction of both the hydrocarbon and hydrogen. It is speculated that the introduction of hydrogen aids in the transformation of the hydrocarbon into other organic precursors which can then be uptaken and catalysed into CNTs.

4. Noble Metal Nanoparticle Catalysts

Nanosized iron-group metals (Fe, Co, Ni) are known for their ability to catalyse SWNT growth in chemical vapour deposition. It has been generally accepted that these metals and their alloys consistently show the highest catalytic activity (Awasthi et al., 2005; Melechko et al., 2005). This is attributed to the solubility of carbon in the metal-solid solution (Deck & Vecchio, 2006). However, noble metals such as Au, Ag or Cu have both negligible carbon solubility and negligible carbide formation, and have recently been identified as catalysts for the growth of CNTs. Takagi et al. (2006) have found that the yield of SWNTs from noble metals is comparable to that of iron-group metals. Moreover, noble metals, in particular Cu, are thought to favour CVD growth of CNT nanotubes at low temperatures with a narrow chirality distribution (Yazyev & Pasquarello, 2008).
Bulk Au is considered a noble metal, as it is highly unreactive and catalytically inactive. Au is the only metal with an endothermic chemisorbtion requirement, and in addition it has *d*-states so low in energy that the interaction with oxygen 2*p*-states is net repulsive. Nevertheless, in its nanoparticle form, Au is capable of catalysing a wide variety of reactions. These include the oxidation of CO (Hvolbaek et al., 2007), the selective hydrogenation of acetylene (Jia et al., 2000), hydrogenation of halogen compounds, reduction of nitrogen oxides and photocatalytic hydrogen production (Haruta, 1997). The origin of this effect is believed to be the increase in the fraction of low-coordinated Au atoms as the size of the Au cluster is reduced. In some cases, the catalytic nature of supported Au clusters can be explained by assuming the Au-support perimeter interface acts as a site for activating at least one of the reactants.
The first demonstration of CNT growth from Au nanoparticle catalysts by Lee et al. (2005), involved the decomposition of acetylene over nanoparticles supported on SiO_2-Al_2O_3. This support showed a good propensity for the decomposition of acetylene and demonstrated

strong interactions between the Au nanoparticles and its surface. The synthesized products were predominantly MWNTs, with average diameters of $\leq$ 20 nm. The first reports of the formation of SWNTs from small Au nanoparticle catalysts were by Takagi et al. (2006) and Bhaviripudi et al. (2007). XPS measurements in both publications showed that CNT growth was only possible from contaminant-free catalyst nanoparticles, once the residual shell of gold oxides or gold chlorides were reduced by H_2. The findings of Liu et al. (2008a) corroborate this finding. Interestingly, neither paper detected any radial breathing modes in the low Raman shift region, corresponding to large diameter nanotubes.

Figure 2(a) shows a scanning electron microscope image of carbon nanotubes synthesized from a Au nanoparticle catalyst. In this experiment, colloidal gold nanoparticles were spin coated on SiO_2 (300 nm) capped Si substrates. Atomic force microscopy (AFM) characterisation of the catalyst revealed that the nanoparticles were approximately 1.4 nm in diameter, with a very narrow particle size distribution, shown in Figure 2(b). The measurements indicated a density of 2500 ± 790 (mean $\pm$ standard deviation) particles/μm^2, which corresponds to an interparticle separation of approximately 20 ± 3 nm. The samples were then pretreated in an H_2 atmosphere for 10 minutes at temperatures ranging from $850 - 1050$ °C, followed by a growth step in a mixture of CH_4 and H_2 at 850 °C. The highest area density was found for samples pretreated at 1000 °C. Raman spectroscopy, with an excitation wavelength of 632.8 nm, was performed in order to evaluate the synthesized nanotubes; a typical spectrum is shown in Figure 2(c). The spectrum exhibits the radial breathing mode feature, indicating that the synthesized nanotubes are predominantly single walled.

From AFM measurements taken to analyse the influence of the pretreatment step on catalyst morphology, we can determine that the initial density of particles is reduced as pretreatment increases. The initial density of 2500 ± 790 particles/μm^2 was reduced to 420 and 290 particles/μm^2 after a pretreatment at 900 °C and 1000 °C, respectively. Broadening of the nanoparticles size distribution is accompanied by a reduction of the modal height as pretreatment temperatures increase. This reduction in density and modal height of the catalyst nanoparticles can be attributed to the evaporation of Au from the substrate in conjuction with the possible diffusion of the Au into the substrate. A similar effect was reported by Bhaviripudi et al. (2007), and may be the cause of the difficulty in synthesizing large diameter nanotubes in other reports. The broadening of the particle size distribution is thought to be owed to particle coalescence by ripening and migration. This change in morphology during pretreatment may even modify the nature of the catalyst surface, thus modifying the catalytic properties of the nanoparticles and consequently the morphology of the carbon products produced (Pisana et al., 2007; Wang et al., 2007).

Typically, the vapour-liquid-solid mechanism is used to explain the mechanism of carbon uptake, supersaturation and precipitation in the catalyst. However, owing to the low solubity of carbon in bulk Au, this must be reviewed for the synthesis of CNTs from Au nanoparticles. By studying the formation of carbon nanowires (CNWs) from Au catalysts, Takagi et al. (2008) inferred that nanosized Au shows some carbon solubility and that Au can form Au-C nanoalloy droplets and produce CNWs by the VLS mechanism. When the catalyst size approaches $\leq$ 5 nm, the carbon solubility and the nanowire nucleation energy increases dramatically, leading to a structural change in the synthesized carbon products from CNW to SWNT. This finding is in agreement with simulations by Yazyev & Pasquarello (2008), who determined that monatomic carbon in Au can diffuse uniformly across the nanoparticle, even at low temperatures. However, it should be noted that no direct evidence of this effect was demonstrated

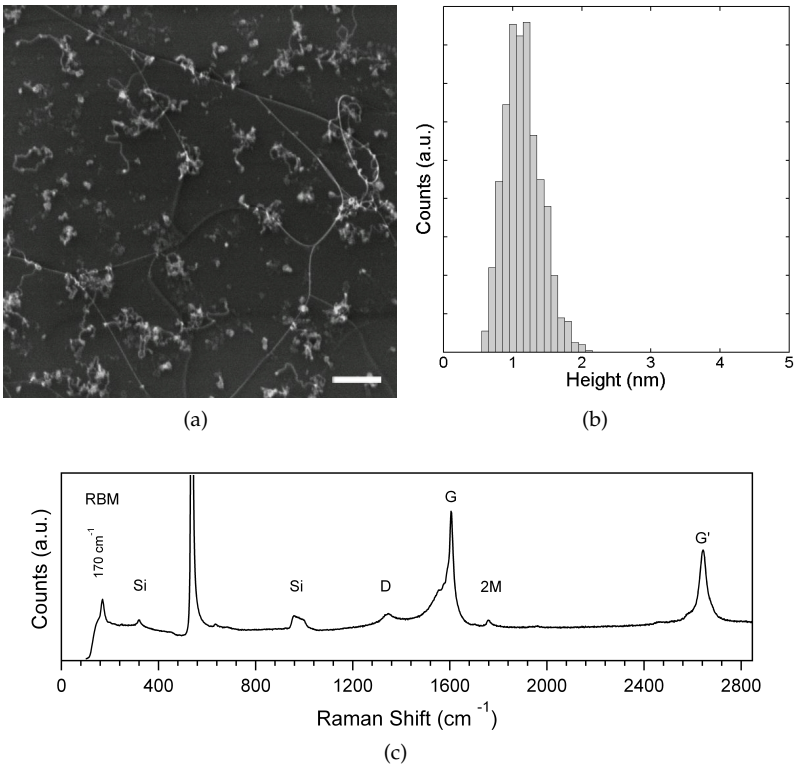

Fig. 2. (a) SEM image of CNTs synthesized from Au nanoparticles pretreated in H_2 at 1000 °C. Scale bar corresponds to 250 nm. (b) Particle size distribution of the as-deposited Au catalyst on a SiO_2 substrate. (c) Typical Raman spectrum from CNTs synthesized from the Au catalyst at the optimum growth condition.

and that similar studies (Yoshihara et al., 2008) could not determine whether carbon atoms were supplied to the nanotube from the Au-C liquid phase or through surface diffusion.

Metallic Cu, long considered to be a contaminant in the growth of SWNTs, has also been reported as an efficient catalyst for SWNT formation in several studies (Takagi et al., 2006; Yuan et al., 2008; Zhou et al., 2006). Figure 3(a) shows a SEM image of CNTs synthesized from a Cu catalyst. In this experiment, Cu nanoparticles were formed by the thermal decomposition of $Cu(NO_3)_2$ in air at 400 °C, deposited from a 1 mM isopropanol solution on a SiO_2 support. The particle size distribution of the catalyst, as determined by AFM, is shown in Figure 3(b). The mean particle size was found to be 1.5 ± 0.4 nm (mean $\pm$ standard deviation), with a particle density 350 ± 50 particles/μm^2. The samples were then pretreated in an H_2 atmosphere for 10 minutes at 900 °C, followed by a growth step in a mixture of CH_4 and H_2 at the same temperature. Raman spectroscopy showed that the synthesized carbon products were predominantly high quality SWNTs (Figure 3(c)).

It has been reported that the carbon solubility in a metallic catalyst should be in the range of $0.5 - 1.5$ wt% carbon in order to efficiently form CNTs (Deck & Vecchio, 2006). Therefore,

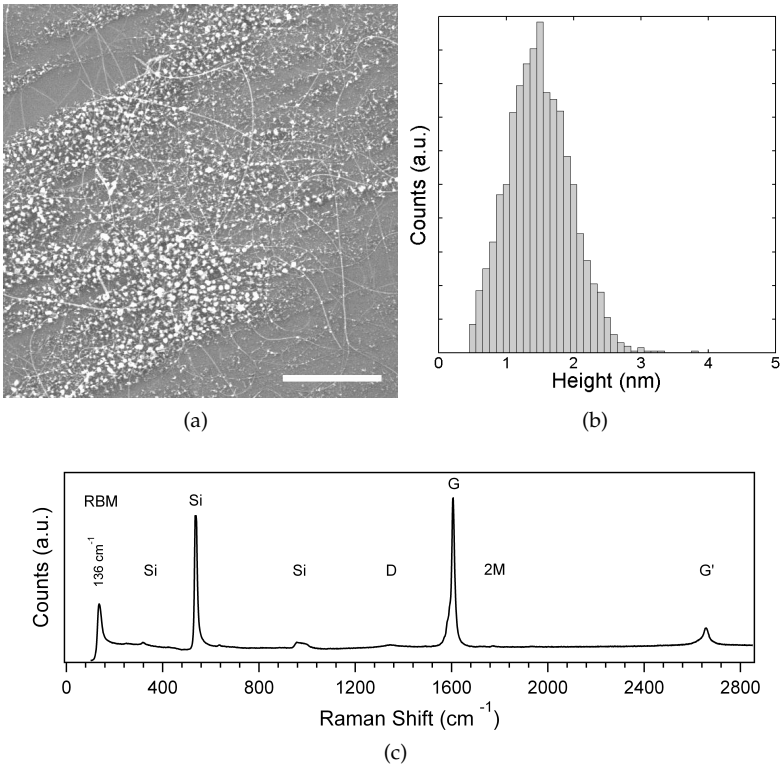

Fig. 3. (a) SEM image of CNTs synthesized from Cu nanoparticles at 900 °C. Cu nanoparticles were fabricated by the thermal decomposition of $Cu(NO_3)_2$, deposited from solution. Scale bar corresponds to 1 μm. (b) Particle size distribution of the decomposed Cu catalyst on a SiO_2 substrate. (c) Typical Raman spectrum from CNTs synthesized from the Cu catalyst at the optimum growth condition.

it is surprising that Cu can be catalytically active, as its carbon solubility is extremely low. However, Zhou et al. (2006) argue that the low solubility of carbon in Cu results in an increased rate of carbon precipitation. Additionally, Cu has a lower catalytic ability for the dissociation of alkanes than traditional catalysts, resulting in a slower supply of carbon in the CVD process. Thus, matching the supply of carbon to the formation rate of nanotubes will result in the production of high quality SWNTs (Lu & Liu, 2006). This argument is supported by Yazyev & Pasquarello (2008), who state that the stability and the diffusion barriers of diatomic carbon on Cu allow one to restrict the diffusion pathways to the nanoparticle surface by choosing an appropriate gas-phase carbon source, resulting in the preferred formation of high quality SWNTs.

Interestingly, Zhou et al. (2006) reported a higher ratio of metallic SWNTs in Cu catalysed samples, determined from Raman analysis. This characteristic was not detected in our experiments. However, only one laser excitation line was used and the sampling size was too small to draw any significant conclusions. Simulations by Yazyev & Pasquarello (2008) also found

that the nucleation of graphitic fragments bound to the Cu nanoparticle catalyst favours the formation of metallic nanotubes. In addition, the low melting point and low carbon diffusion barriers suggest that CVD synthesis could take place at much lower temperatures. In these conditions, the chirality preference would be further enhanced.

5. Semiconductor Nanoparticle Catalysts

Results presented in the previous sections demonstrate that hydrocarbon dissociation and graphite formation abilities are not essential in a catalyst to synthesize CNTs. This leads to a new interpretation of the role of the catalyst particle in CNT growth, where only a nanoscale curvature is needed to act as a template for nanotube formation. This assertion is supported by the reports of CNT formation from semiconductor nanoparticles (Takagi et al., 2007; Uchino et al., 2009; 2008; 2005b), from which no catalytic functions were expected.

The first reports of CNT growth from semiconducting catalysts were by Uchino et al. (2005b). In this experiment, carbon-doped SiGe islands, deposited by CVD on Si, form nanoscale clusters through various mechanisms which act as a seed for SWNT growth. These results were supported by the work of Takagi et al. (2007), who showed that CNT growth from Ge, Si and SiC nanoparticles was possible. More recently, there have been various reports of CNT growth from SiO_2 nanoparticles (Huang et al., 2009; Liu et al., 2009), which are thought to be promising catalysts owing to their ability to maintain a narrow size distribution at CNT growth temperatures.

In this section, research on the use of germanium for carbon nanotube growth is reviewed. Four different techniques to synthesize CNTs based upon Ge nanoparticle catalysts are investigated. These are based on SiGe islands, Ge Stranski-Krastanow dots, Ge nanoparticles formed by ion implantation and colloidal Ge nanoparticles. It is shown that in all cases high quality SWNTs can be grown.

5.1 SiGe Islands

A 50 nm thick $Si_{0.7}Ge_{0.3}$ layer was deposited by CVD on Si(001) wafers after the growth of a thin Si buffer layer. To accommodate the stress resulting from the lattice mismatch between Si and Ge, the SiGe layer forms islands on top of a thin wetting layer. The heights of the islands ranged from 20 to 50 nm. Subsequently, the islands were implanted with carbon ions (energy 30 keV, dose of 3×10^{16} cm^{-2}). This heavy ion implantation is thought to induce damage and form an amorphous layer at the surface (Uchino et al., 2005a). The substrates were then dipped in buffered HF solution to remove the native oxide. Chemical oxidation was performed using a 30% hydrogen peroxide (H_2O_2) solution at room temperature. This step was followed by a pretreatment step in a mixture of Ar and H_2 for 10 minutes at 900 °C, followed by the CNT growth step in a mixture of CH_4 and H_2 at 850 °C.

Figure 4(a) shows a SEM image of the as-synthesized products on SiGe islands. In this image, two distinct types of nanostructures are visible. The short and thick nanofibres, approximately 20 nm in diameter and 1 μm in length, are formed during the pretreatment step. These nanostructures were identified as SiO_x nanowires by TEM, Raman and photoluminescence measurements, and are formed by the carbothermic reduction of SiO_2 (Lee et al., 2004; Li et al., 2004). These fibres were easily removed by an HF vapour etch, as shown in Figure 4(b). The second type of nanostructure forms during the growth step and comprises straight and thin fibres of less than 10 nm diameter and approximately 5 μm in length. Raman measurements, shown in Figures 4(c) and 4(d), confirm that these fibres are SWNTs. Despite considerable effort, the disorder induced D-band feature that is normally seen at 1350 cm^{-1} (Dresselhaus

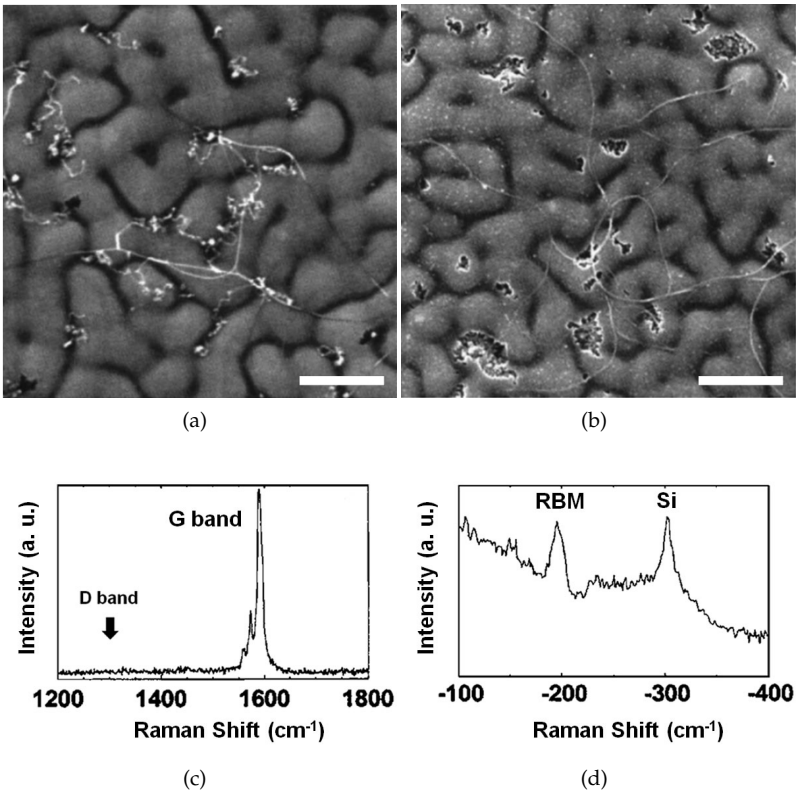

Fig. 4. SEM images of as grown CNTs and SiO_x nanowires synthesized from C implanted SiGe islands (a) before and (b) after HF vapour etching, showing that only carbon nanotubes remain. Scale bar corresponds to 500 nm. Typical Raman spectra of the as-grown CNTs showing (c) G-band characteristic and (d) anti-Stokes spectra showing the radial breathing mode characteristic.

et al., 2005) could not be detected. This indicates that the nanotubes have a low defect density, and thus could be described as high quality.

In this experiment, nanoscale Ge clusters are formed following the chemical oxidation and annealing of the SiGe layers. The oxidation behaviour of SiGe layers has been studied to a great extent (Liou et al., 1991; Paine et al., 1991). Si is known to have a stronger thermodynamic tendency to be oxidised in comparison to Ge. Therefore, the dry oxidation of SiGe alloys, with a low Ge content, results in the formation of SiO_2 and the segregation of Ge clusters from the growing oxide (Sass et al., 2002). It should be noted that this effect is less pronounced with wet oxidation, and the oxide layer typically contains a mixture of Si-O and Ge-O bonds. However, upon annealing in a reducing atmosphere, the Ge-O bonds are preferentially broken owing to a lower stability, resulting in the formation of nanoscale Ge clusters (Paine et al., 1993). These clusters are thought to act as the catalyst for the growth of CNTs in this methodology.

5.2 Ge Stranski-Krastanow Dots

Figure 5(a) shows a TEM image of a bundle of SWNTs grown from Ge Stranki-Krastanow dots. In this experiment, Ge Stranski-Krastanow dots are formed by CVD deposition of Ge atop a thin Si buffer layer. This step forms Ge dots in the form of cones with diameters from 20 to 250 nm and heights between 10 and 25 nm. Subsequently, the islands were implanted with carbon ions (energy 30 keV, dose of 3×10^{16} cm^{-2}). The substrates were then dipped in buffered HF solution to remove the native oxide and subjected to a chemical oxidation using a 30% hydrogen peroxide (H_2O_2) solution at room temperature. This step was followed by a pretreatment step in a mixture of Ar and H_2 for 10 minutes at 900 °C, followed by the CNT growth step in a mixture of CH_4 and H_2 at 850 °C. Raman measurements on the synthesized CNTs (Figure 5(b)) clearly show the radial breathing mode feature and tangential G band mode expected for SWNTs. The radial breathing modes indicate that the diameters of the synthesized CNTs are in the range 1.6 to 2.1 nm, which are slightly larger than those on SiGe islands (Uchino et al., 2005b). Again, the disorder induced D-band could not be detected, indicating that these CNTs are of a high quality.

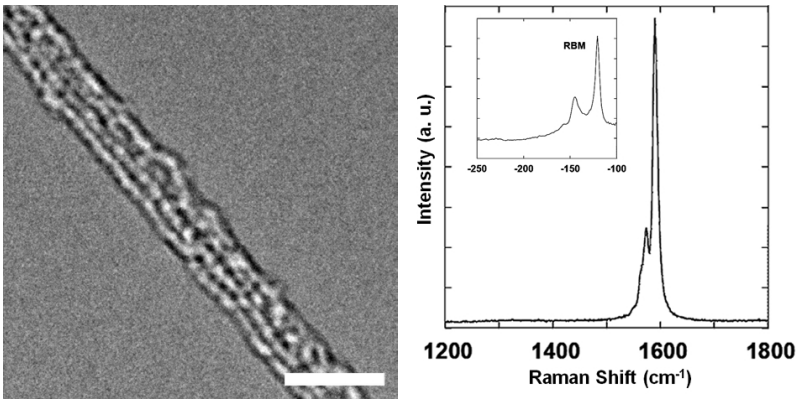

(a) (b)

Fig. 5. (a) TEM image of a bundle of SWNTs synthesized from C implanted Ge Stranski-Krastanow dots. Scale bar corresponds to 10 nm. The TEM sample was prepared by scraping the substrate surface with a surgical blade and collecting the material on a holey-carbon TEM grid. (b) Typical Raman spectra of the as-grown CNTs showing the G-band characteristic. Inset shows anti-Stokes spectra displaying the radial breathing mode characteristic.

It is believed that the mechanism of formation is very similar to that of the CNTs grown from SiGe islands. Upon chemical oxidation of the Ge Stranski-Krastanow dots, a thin layer of SiGe oxide is formed. Following a subsequent anneal in a reducing atmosphere, Ge clusters are nucleated and it is believed that these act as catalysts in this growth technique. Sass et al. (2002) reported that after the oxidation of Ge islands on Si(001), recovery of the original dot structure was not possible. Instead, a reduction of the GeO_2 around the single crystalline core of the non-oxidized Ge dot materials results in only Ge-enriched clouds, surrounded by a matrix of non-reductible material. This assertion is supported by SEM images taken after each stage in the process (not shown), which indicate a definite change of morphology after the chemical oxidation and reduction steps (Uchino et al., 2008). In fact, there have been

reports of the formation of ultra-high density Ge nanoparticles, with diameters of about 4 nm, from the oxidation/reduction of Ge/Si surfaces (Nakamura et al., 2004), which further supports this hypothesis.

5.3 Ge Nanoparticles fabricated by Ion Implantation

In order to further investigate the role of Ge nanoparticles in the growth of carbon nanotubes, Ge nanoparticles were fabricated directly by Ge ion implantation into a layer of thermally oxidised SiO_2, and subsequently annealed at 600 °C. This step was followed by a HF vapour etch to remove the SiO_2 and expose the Ge nanoparticles. AFM characterisation revealed that a uniform layer of nanoparticles had been synthesized with a mean density of 460 ± 30 particles/μm^2 and a modal height of 1.8 nm. The particle size distribution is shown in Figure 6(a). This result shows good agreement with others in the literature, for instance Min et al. (1996) reported the formation of Ge nanocrystals by a similar process, with an average size of 1.9 ± 0.8 nm. Selected samples were then implanted with C. The C implanted samples showed a lower particle density (70 ± 18 particles/μm^2), a lower modal height (0.7 nm), and a narrower size distribution, shown in Figure 6(b). This change in morphology is attributed to a sputtering effect caused by the ion implantation.

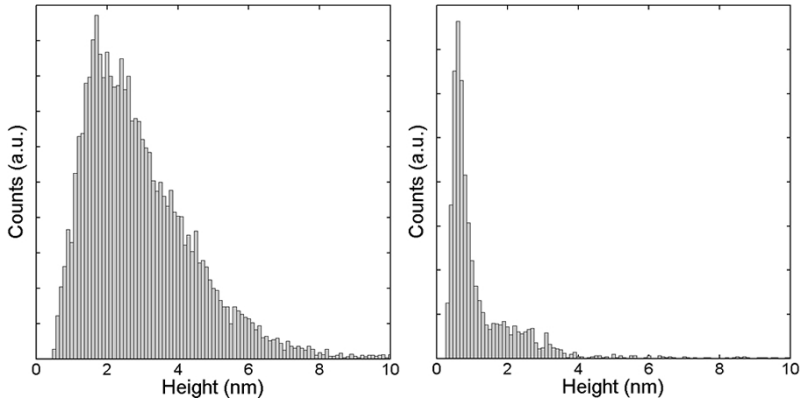

Fig. 6. (a) AFM particle size distributions of Ge nanoparticles synthesized by Ge ion implantation (20 keV, 5×10^{15} cm^{-2}) into a 30 nm thick SiO_2 layer and annealed at 600 °C for 40 min in N_2 followed by an HF vapour etch to expose the nanoparticles. (b) AFM particle size distribution for samples given a C implant (30 keV, 3×10^{16} cm^{-2})

Figure 7(a) and 7(b) shows a typical SEM image after CNT growth for a sample without and with C implantation, respectively. Both images show that a good density of CNTs are achievable using this methodology. Representative Raman spectra for samples without and with C implantation are shown in Figure 7(c) and 7(d), respectively. All samples (insets) clearly show the radial breathing mode, indicating that single walled nanotubes are present. In the case of CNTs grown without C implantation, a small D-band peak is visible around 1320 cm^{-1}, which can be attributed to disorder in the nanotubes. In contrast, samples grown from the C implanted samples show no D-band peak. This indicates that the SWNTs synthesized from C implanted Ge nanocrystals have a low defect density, and are thus high quality.

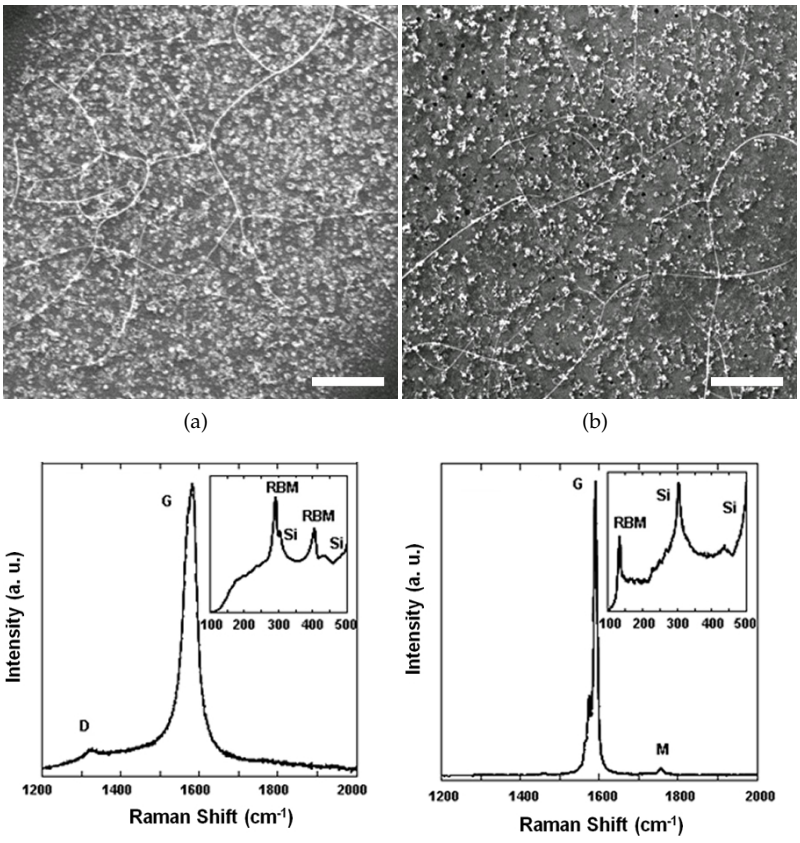

Fig. 7. SEM images of CNTs grown from Ge nanoparticles fabricated by ion implantation from (a) nonimplanted samples and (b) carbon implanted samples. Scale bar corresponds to 500 nm. Typical Raman spectra of the as-grown CNTs from (c) nonimplanted and (d) carbon implanted Ge nanocrystals. Inset shows Stokes spectra displaying the radial breathing mode characteristic.

At the optimum growth condition, there is no statistically significant benefit in terms of area density from the C implant. However, results at other growth conditions show that successful CNT growth can be achieved for a wider range of temperatures when the C implant is formed. AFM measurements taken to analyse the influence of the pretreatment temperature revealed that samples without a C implant show a strong reduction in particle density with increasing pretreatment temperature. In contrast, samples with a C implant show a much smaller decrease in particle density with increasing pretreatment temperature. This suggests that the C implant might increase the Ge melting point through formation of a $Ge_{1-y}C_y$ alloy. This hypothesis is supported by the phase diagram of the Ge-C system presented by Scace & Slack

(1959), which indicates that the presence of a small percentage of C has a strong effect in raising the melting point of Ge. Furthermore, Kanazawa et al. (2001) demonstrate that $Ge_{1-y}C_y$ alloys can be successfully formed by C implantation into Ge.

5.4 Colloidal Germanium Nanoparticles

Figure 8(a) shows an AFM image of Ge nanoparticles deposited from a 1mM colloidal solution on a SiO_2 support by spin coating. The colloidal solution was synthesized by means of an inverse micelle method. The synthesis of a $Ge[N(SiCH_3)_2]_2$ precursor for the formation of Ge nanocrystals was based on the works of Lessing et al. (1977a;b), with some minor modifications. The precursor (50mg) was dissolved in 7 ml of trioctylamine and injected into hot (340 °C), molten hexadecylamine (HDA, 1g). The injection method was inspired from various publications and has been standardised for this purpose (Nair et al., 2002, and references therein). The residue was then dissolved in toluene, re-precipitated with methanol and suspended in tryoctlamine. This process yielded nanoparticles with a narrow size distribution, shown in Figure 8(b). The synthesized nanoparticles had a mean size of 1.5 ± 0.4 nm, and the density of the spin coated layer was 430 ± 60 particles/μm^2.

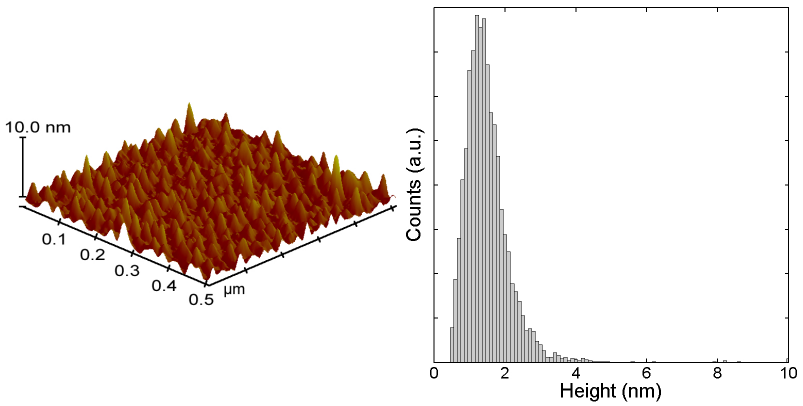

(a) (b)

Fig. 8. (a) AFM image and (b) particle size distributions of colloidal Ge nanoparticles, deposited on SiO_2 by spin coating of a 1 mM solution. After deposition, samples were cleaned in a 100W O_2 plasma for 30 minutes.

Samples were then subjected to a 100W O_2 plasma for 30 minutes in order to remove the organic residue left from deposition. Subsequently, samples were pretreated in an H_2 atmosphere for 10 minutes at temperatures ranging from $850 - 1050$ °C, followed by a growth step in a mixture of CH_4 and H_2 at 850 °C. The highest area density was found for samples pretreated at 900 °C, shown in Figure 9(a). Raman spectroscopy showed that the synthesized carbon products were predominantly high quality SWNTs (Figure 9(c)). Synthesis on sapphire (Al_2O_3) substrates showed that a slightly higher uniformity and area density of CNTs was achievable on this support medium, shown in Figure 9(b). This is attributed to the ability of the Al_2O_3 support to provide an interface for graphite formation (Rummeli et al., 2007).
In comparison to the non C implanted Ge nanoparticles fabricated by ion implantation, the process window for this methodology was considerably wider, with little change in CNT area

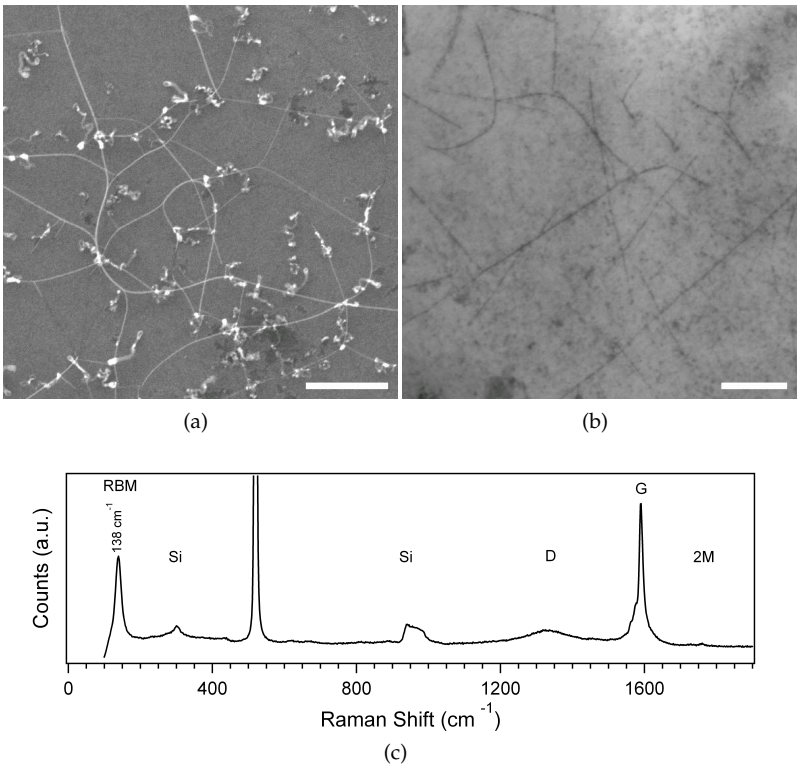

Fig. 9. SEM image of CNTs synthesized from colloidal Ge nanoparticles pretreated at 900 °C in H_2, followed by a CNT growth step at 850 °C in a mixture of CH_4 and H_2 on a (a) SiO_2 support and a (b) sapphire (Al_2O_3) support. Scale bar corresponds to 500 nm in both images. (c) Typical Raman spectrum from CNTs synthesized from the colloidal Ge catalyst at the optimum growth condition.

density in samples pretreated at temperatures from 900 to 1000 °C. AFM studies of the catalyst after H_2 pretreatment revealed that there was no statistically significant reduction in particle density with increasing pretreatment temperature. In addition, rather than a reduction in mean particle size, a very slight increase in size was found with increasing pretreatment temperature. This effect is believed to be due to the organic cap on the nanoparticles acting as a stabilising agent as the furnace ramps up to temperature. It should be noted that at the synthesis temperatures, the organic cap on the nanoparticles is expected to be fully reduced.

6. Growth Mechanism Discussion

Despite enormous strides in the synthesis of carbon nanotubes, the mechanism for growth is still a highly debated issue. As discussed previously, it is generally accepted that the model for carbon filament growth (Baker, 1989; Baker et al., 1972; 1973), derived from concepts of vapour-liquid-solid theory, also applies to carbon nanotube growth. This belief arises from

the visual observation (by TEM) of catalyst particles on the ends of nanotubes, as was the case with carbon filaments. In this model, hydrocarbons adsorbed on the metal nanoparticle are catalytically decomposed resulting in atomic carbon dissolving into the liquid catalyst particle, and when a supersaturated state is reached, carbon precipitates in a tubular, crystalline form.

However, the results presented in this work suggest that this belief holds several observational inconsistencies that do not support this mechanism for CVD production. The successful CNT growths from catalyst free, noble metal catalysts and semiconducting catalysts imply that hydrocarbon dissociation ability is not essential in a catalyst. It should be noted that the catalytic behaviour of Cu and Au may be explained by electron donation to the support (Vander Wal et al., 2001), creating *d*-vacancies which may cause hydrocarbon dissocation. However, the ability of catalyst-free and semiconducting catalysts to seed CNT growth cannot be explained by the same mechanism. Reilly & Whitten (2006) argue that a more likely scenario is that a free radical condensate (FRC) provides carbon species through a leaving group, such as hydrogen (or oxygen). FRCs naturally form during hydrocarbon pyrolysis by the breaking of carbon-hydrogen or carbon-carbon bonds with each fragment keeping one electron to form two radicals. The presence of a radical in a hydrocarbon molecule permits rapid rearrangement of carbon bonds. In this case, the catalyst particle's role is to simply provide an interface where carbon rearrangement can occur and act as a template for growth.

Typically, metal catalysts with no *d*-vacancies, such as Cu and Au, do not offer sites to dissolve carbon, such that neither saturation nor precipitation is possible. However, despite the low carbon solubility, these catalysts have demonstrated an ability to catalyse CNT formation. Additionally, catalysts with a high melting point such as Al_2O_3 or ZrO_2 are thought to be solid at CNT synthesis temperatures. However, if nanoparticles of these metals are small enough ($\leq$ 5 nm), the increasing fraction of low-coordinated atoms may lead to surface saturation followed by carbon precipitation, as reported by Takagi et al. (2006). Considering that carbon penetration inside small nanoparticles is unlikely (Raty et al., 2005), the growth of CNTs is most likely a process primarily controlled by surface diffusion (Chadderton & Chen, 1999; Ding et al., 2005). Indeed, it is believed by several groups that the rate-limiting factor in CNT synthesis is the surface diffusion of carbon across the catalyst (Bartsch et al., 2005; Hofmann et al., 2005). Additionally, this factor could explain the influence of the carbon source on the ability of a catalyst to synthesize CNTs. Yazyev & Pasquarello (2008) reported different activation energies for the surface diffusion of C dimers and adatoms on noble metal catalysts, and argued that appropriate choice of a diatomic or monatomic carbon gas-phase source could significantly accelerate diffusion.

The specificity of the growth of nanotubes on nanoparticles with regard to the growth of carbon filaments is their nanometer dimensions. Other mechanisms are therefore required to explain the nucleation of CNTs from nanoparticle catalysts. One such model is the Yarmulke mechanism proposed by Dai et al. (1996). In the Yarmulke mechanism, a graphene cap is assembled on the particle surface with its edges strongly chemisorbed to the catalyst. The graphene cap acts to reduce the high total surface energy of the particle caused by its high curvature, owing to the fact that the basal plane of graphite has an extremely low surface energy. As additional carbon atoms are added, the hemifullerene cap formed on the particle surface lifts off, creating a hollow tube with constant diameter which grows away from the particle (Nikolaev et al., 1999). This model was supported by molecular dynamics simulations by Shibuta & Maruyama (2003). Recent works in high-resolution *in-situ* TEM observation of the catalytic growth of CNTs have verified this mechanism (Helveg et al., 2004; Hofmann et al.,

2007). These studies have also shown that cap stabilisation and nanotube growth involve reshaping of the catalyst nanoparticle.

7. Conclusions and Future Directions

In this review, the role of the catalyst in the selective growth of SWNTs by CVD has been studied. Evidence of self-assembled carbon nanostructures was presented, indicating that upon annealing, C undergoes a structural reorganization to form graphitic structures. In addition, SWNT growth was shown to be possible from ceramic, noble metal and semiconducting catalysts. This demonstrates that hydrocarbon dissociation and graphitization ability are not essential in a catalyst, and it was argued that carbon species are supplied through a free radical condensate. The results presented show that the commonly utilised model of carbon filament growth is inadequate to describe SWNT growth from non traditional catalysts. A new interpretation of the role of the catalyst was presented where only a nanoscale curvature is necessary to grow CNTs. A mechanism for SWNT growth was suggested where the surface saturation and diffusion of C on the catalyst nanoparticle lead to the formation of a graphitic cap followed by the further incorporation of C into a growing nanotube.

Although there have been tremendous advances in the fabrication of CNTs, the integration of these nanostructures into successful applications and large-scale production processes depend on the understanding of several fundamental issues, which are yet to be addressed. A few of these issues are briefly discussed below.

The role played by the support in the CVD of CNTs is not yet fully understood. The simplistic view that the support only plays a catalytically passive role in the formation of CNTs requires examination. The work of Rummeli et al. (2007) demonstrated that under typical CVD growth conditions, nanoparticles of difficult-to-reduce metal oxides were capable of promoting ordered carbon growth. The authors attributed this to the presence of surface defect sites on the nanoparticle oxides. However, the interface between the catalyst nanoparticle and the support is thought to act as a annular defect site. This would indicate that the nature of the support-nanoparticle interface may be very important to the behaviour of the catalyst.

There appears to be a consensus in the literature concerning the correlation of catalyst size and SWNT diameter. Several groups have observed a direct dependence of the two quantities (Jeong et al., 2005; Wei et al., 2001). However, whether there is a correlation between the atomic structure/facets of the nanoparticle catalyst and the chirality of the synthesized nanotube has not yet been determined. If a good correlation is found between the facets and the chirality of the nanotube, how can the physical structure of the nanoparticles be retained as the sample is heated to the synthesis temperature?

The low-temperature synthesis of CNTs is of significant technological importance. This is essential for synthesis on glass substrates or other applications requiring plastic substrates. However, it is not yet clear whether this is possible and what the effect on the material quality would be. The integration of carbon nanotubes in IC manufacturing would also require large area growth uniformities, however most research is undertaken in small, low-throughput batch reactors, typically on small pieces of wafers. This is expected to change as the market for CNT-based products begins to emerge, creating the need for large-scale commercial reactors.

8. References

Awasthi, K., Srivastava, A. & Srviastava, O. N. (2005). Synthesis of Carbon Nanotubes, *J. Nanosci. Nanotechnol.* **5**: 1616–1636.

Baker, R. T. K. (1989). Catalytic Growth of Carbon Filaments, *Carbon* **27**: 315.

Baker, R. T. K., Barber, M. A., Harris, P. S., Feates, F. S. & White, R. J. (1972). Nucleation and Growth of Carbon Deposites from the Nickel Catalyzed Decomposition of Acetylene, *J. Catal.* **26**: 51.

Baker, R. T. K., Harris, P. S., Thomas, R. B. & Waite, R. J. (1973). Formation of Filamentous Carbon from Iron, Cobalt and Chromium Catalyzed Decomposition of Acetylene, *J. Catal.* **30**: 86.

Bartsch, K., Biedermann, K., Gemming, T. & Leonhardt, A. (2005). On the Diffusion-Controlled Growth of Multiwalled Carbon Nanotubes, *J. Appl. Phys.* **97**: 114301.

Berger, L.-M., Gruner, W., Langholf, E. & Stolle, S. (1999). On the Mechanism of Carbothermal Reduction Processes of TiO_2 and ZrO_2, *Int. J. Refract. Met. Hard Mater.* **17**: 235–243.

Bhaviripudi, S., Mile, E., Steiner, S. A., Zare, A. T., Dresselhaus, M. S., Belcher, A. M. & Kong, J. (2007). CVD Synthesis of Single-Walled Carbon Nanotubes from Gold Nanoparticle Catalysts, *J. Am. Chem. Soc.* **129**: 1516–1517.

Botti, S., Asilyan, C. R. L., Dominicis, L. D., Fabbri, F., Orlanducci, S. & Fiori, A. (2004). Carbon Nanotubes Grown by Laser-annealing of SiC Nano-particles, *Chem. Phys. Lett.* **400**: 264–267.

Botti, S., Asilyan, L. S., Ciardi, R., Fabbri, F., Lortei, S., Santoni, A. & Orlanducci, S. (2001). Catalyst-Free Growth of Carbon Nanotubes by Laser Annealing of Amrphous SiC Films, *Chem. Phys. Lett.* **396**: 1–5.

Botti, S., Ciardi, R., Terranova, M. L., Piccirillo, S., Sessa, V., Rossi, M. & Vittori-Antisari, M. (2002). Self-Assembled Carbon Nanotubes Grown Without Catalyst From Nanosized Carbon Particles Adsorbed on Silicon, *Appl. Phys. Lett.* **80**: 1441.

Chadderton, L. T. & Chen, Y. (1999). Nanotube Growth by Surface Diffusion, *Phys. Lett. A* **263**: 401–405.

Dai, H., Rinzler, A. G., Nikolawv, P., Thess, A., Colbert, D. T. & Smalley, R. E. (1996). Single-wall Nanotubes Produced by Metal-Catalyzed Disproportionation of Carbon Monoxide, *Chem. Phys. Lett.* **260**: 471–475.

Deck, C. P. & Vecchio, K. (2006). Prediction of Carbon Nanotube Growth Success by the Analysis of Carbon-Catalyst Binary Phase Diagrams, *Carbon* **43**: 2654–2663.

Derycke, V., Martel, R., Radosavljevic, M., Ross, F. M. & Avouris, P. (2002). Catalyst Free Growth of Ordered Single Walled Carbon Nanotube Networks, *Nano Lett.* **2**: 1043–1046.

Ding, F., Rosen, A. & Bolton, K. (2005). Dependence of SWNT Growth Mechanism on Temperature and Catalyst Particle Size: Bulk versus Surface Diffusion, *Carbon* **43**: 2215–2217.

Dresselhaus, M. S., Dresselhaus, G., Sait, R. & Jorio, A. (2005). Raman Spectroscopy of Carbon Nanotubes, *Phys. Rep.* **409**: 47.

Haruta, M. (1997). Size- and Support-Dependency in the Catalysis of Gold, *Catal. Today* **36**: 156–166.

Helveg, S., Lopez-Cartes, C., Sehested, J., Hansen, P. L., Clausen, B. S., Rostrup-Nielsen, J. R., Abild-Pedersen, F. & Norskov, J. K. (2004). Atomic-scale Imaging of Carbon Nanofibre Growth, *Nature* **427**: 426–429.

Hofmann, S., Csányi, G., Ferrari, A. C., Payne, M. C. & Robertson, J. (2005). Surface Diffusion: The Low Activation Energy Path for Nanotube Growth, *Phys. Rev. Lett.* **95**: 036101.

Hofmann, S., Sharma, R., Ducati, C., Du, G., Mattevi, C., Cepek, C., Cantoro, M., Pisana, S., Parvez, A., Cervantes-Sodi, F., Ferrari, A. C., Dunin-Borkowski, R., Lizzit, S., Petaccia, L., Goldoni, A. & Robertson, J. (2007). In situ Observations of Catalyst Dynamics during Surface-Bound Carbon Nanotube Nucleation, *Nano Lett.* **7**: 602–608.

Huang, S., Cai, Q., Chen, J., Qian, Y. & Zhang, L. (2009). Metal-Catalyst-Free Growth of Single-Walled Carbon Nanotubes on Substrates, *J. Am. Chem. Soc.* **131**: 2094–2095.

Hvolbaek, B., Janssens, T. V. W., Clausen, B. S., Falsig, H., Christensen, C. H. & Norkov, J. K. (2007). Catalytic Activity of Au Nanoparticles, *Nano Today* **2**: 14–18.

Iijima, S. (1991). Helical Microtubules of Graphitic Carbon, *Nature* **354**: 56.

Jeong, G.-H., Suzuki, S., Kobayashi, Y., Yamazaki, A., Yoshimura, H. & Homma, Y. (2005). Effect of Nanoparticle Density on Narrow Diameter Distribution of Carbon Nanotubes and Particle Evolution During Chemical Vapour Deposition, *J. Appl. Phys.* **98**: 124311.

Jia, J., Haraki, K., Kondo, J. N., Domen, K. & Tamaru, K. (2000). Selective Hydrogenation of Acetylene over Au/Al_2O_3 Catalyst, *J. Phys. Chem. B* **104**: 1153–1156.

Kanazawa, Y., Katayama, K., Nozawa, K., Saitoh, T. & Kubo, M. (2001). Preparation of $Ge_{1-y}C_y$ Alloys by C Implantation into Ge Crystal and Their Raman Spectra, *Jpn. J. Appl. Phys.* **40**: 5880.

Koshio, A., Yudasaka, M. & Iikima, S. (2002). Metal-free Production of High-Quality Multi-Wall Carbon Nanotubes, in which the Innermost Nanotubes Have a Diameter of 0.4 nm, *Chem. Phys. Lett.* **356**: 595–600.

Kusonoki, M., Rokkak, M. & Suzuki, T. (1997). Epitaxial Carbon Nanotube Fil Self Organised by Sublimation Decomposition of Silicon Carbide, *Appl. Phys. Lett.* **71**: 2620.

Larciprete, R., Lizzit, S., Botti, S., Cepek, C. & Goldini, A. (2002). Structural Reorganisation of Carbon Nanoparticles into Single-Walled Nanotubes, *Phys. Rev. B.: Condes. Matter Mater. Phys.* **66**: 121402.

Larciprete, R., Lizzit, S., Cepek, C., Botti, S. & Goldini, A. (2003). Thermal Reactions at the Interface between Si and C Nanoparticles: Nanotube Self-Assembling and Transformation into SiC, *Surf. Sci.* **532**: 886–891.

Lee, K.-H., Yang, H. S., Baik, K. H., Bang, J., Vanfleet, R. R. & Sigmund, W. (2004). Direct Growth of Amorphous Silica Nanowiresby Solid State Transformation of SiO_2 Films, *Chem. Phys. Lett.* **383**: 380.

Lee, S. Y., Yamada, M. & Miyake, M. (2005). Synthesis of Carbon Nanotubes Over Gold Nanoparticle Supported Catalysts, *Carbon* **43**: 2654–2663.

Lessing, J. G. V., Fouche, K. F. & Retief, T. T. (1977a). Redox Extractions from Molten Alkali-Metal Cyanides. Part 1. Mechanism for Extractions with Liquid Zinc Alloys, *Dalton Trans.* **20**: 2020.

Lessing, J. G. V., Fouche, K. F. & Retief, T. T. (1977b). Redox Extractions from Molten Alkali-metal Cyanides. Part 2. Mechanism for Extractions with Liquid Tin Alloys, *Dalton Trans.* **20**: 2004.

Li, S.-H., Zhu, X.-F. & Zhao, Y.-P. (2004). Carbon-Assisted Growth of SiO_x Nanowires, *J. Phys Chem. B* **108**: 17032.

Liou, H. K., Mei, P., Gennser, U. & Yang, E. S. (1991). Effects of Ge Concentration on SiGe Oxidation Behavior, *Appl. Phys. Lett.* **59**: 1200.

Liu, B., Ren, W., Gao, L., Li, S., Pei, S., Liu, C., Jiang, C. & Cheng, H.-M. (2009). Metal-Catalyst-Free Growth of Single-Walled Carbon Nanotubes, *J. Am. Chem. Soc.* **131**: 2082–2083.

Liu, H., Takagi, D., Ohno, H., Chiashi, S., Chokan, T. & Homma, Y. (2008a). Effect of Ambient Gas on the Catalytic Properties of Au in Single Walled Carbon Nanotube Growth, *Jpn. J. Appl. Phys.* **47**: 1966–1970.

Liu, H., Takagi, D., Ohno, H., Chiashi, S., Chokan, T. & Homma, Y. (2008b). Growth of Single Walled Carbon Nanotubes from Ceramic Particles by Alcohol Chemical Vapor Deposition, *Appl. Phys. Express* **1**: 014001.

Lu, C. & Liu, J. (2006). Controlling the Diameter of Carbon Nanotubes in Chemical Vapor Deposition Method by Carbon Feeding, *J. Phys. Chem. B* **110**: 20254.

Mctaggart, F. K. (1961). Reduction of Zirconium and Hafnium Oxides, *Nature* **191**: 1192.

Melechko, A. V., Merlukov, V. I., McKnight, T. E., Guillorn, M. A., Lowndes, D. H. & Simpson, M. L. (2005). Vertically Aligned Carbon Nanofibers and Related Structures: Controlled Synthesis and Directed Assembly, *J. Appl. Phys.* **97**: 041301.

Meyyappan, M., Yamada, T., Sarrazin, P. & Li, J. (2005). *Carbon Nanotubes: Science and Applications*, CRC Press.

Min, K. S., Shcheglov, K. V., Yang, C. M., Atwater, H. A., Brongersma, M. L. & Polman, A. (1996). The Role of Quantum-Confined Excitons vs Defects in the Visible Luminescence of SiO_2 Films Containing Ge Nanocrystals, *Appl. Phys. Lett.* **68**: 2511.

Nair, P. S., Radhakrishnan, T., Revaprasadu, N., Kolawolea, G. & OŠBrien, P. (2002). Cadmium Ethylxanthate: A Novel Single-Source Precursor for the Preparation of CdS Nanoparticles, *J. Mater. Chem.* **12**: 2722.

Nakamura, Y., Nagadomi, Y., Sugie, K., Miyata, N. & Ichikawa, M. (2004). Formation of Ultrahigh Density Ge Nanodots on Oxidized Ge/Si(111) Surfaces, *J. Appl. Phys.* **95**: 5014.

Nikolaev, P., Bronikowski, M. J., Bradley, R. K., Rohmund, F., Colbert, D. T., Smith, K. A. & Smalley, R. E. (1999). Gas-Phase Catalytic Growth of Single-Walled Carbon Nanotubes from Carbon Monoxide, *Chem. Phys. Lett.* **313**: 91–97.

Paine, D. C., Caragianis, C., Kim, T. Y., Shigesato, Y. & Ishahara, T. (1993). Visible Photoluminescence from Nanocrystalline Ge Formed by H_2 Reduction of $Si_{0.6}Ge_{0.4}O_2$, *Appl. Phys. Lett.* **62**: 2842.

Paine, D. C., Caragianis, C. & Schwartzman, A. F. (1991). Oxidation of $Si_{1x}Ge_x$ Alloys at Atmospheric and Elevated Pressure, *J. Appl. Phys.* **70**: 5076.

Pisana, S., Cantoro, M., Parvez, A., Hofmann, S., Ferrari, A. C. & Robertson, J. (2007). The Role of Precursor Gases on the Surface Restructuring of Catalyst Films During Carbon Nanotube Growth, *Physica E* **37**: 1.

Raty, J.-Y., Gygi, F. & Galli, G. (2005). Growth of Carbon Nanotubes on Metal Nanoparticles: A Microscopic Mechanism from *Ab-Initio* Molecular Dynamics , *Phys. Rev. Lett.* **95**: 096103.

Reich, S., Li, L. & Robertson, J. (2006). Control the Chirality of Carbon Nanotubes by Epitaxial Growth, *Chem. Phys. Lett.* **421**: 469.

Reilly, P. T. A. & Whitten, W. B. (2006). The Role of Free Radical Condensates in the Production of Carbon Nanotubes During the Hydrocarbon CVD Process, *Carbon* **44**: 1653–1660.

Rummeli, M. H., Kramberger, C., Gruneis, A., Ayala, P., Gemming, T., Buchner, B. & Pichler, T. (2007). On the Graphitization Nature of Oxides for the Formation of Carbon Nanostructures, *Chemistry of Meterials* **19**: 4105–4107.

Sass, T., Zela, V., Gustafsson, A., Pietzonka, I. & Seifert, W. (2002). Oxidation and Reduction Behavior of Ge-Si Islands, *Appl. Phys. Lett.* **81**: 3455.

Scace, R. I. & Slack, G. A. (1959). Solubility of Carbon in Silicon and Germanium, *J. Chem. Phys.* **30**: 1551.

Shibuta, Y. & Maruyama, S. (2003). Molecular Dynamics Simulation of Formation Process of Single-Walled Carbon Nanotubes by CCVD Method, *Chem. Phys. Lett.* **382**: 381–386.

Steiner, S. A., Baumann, T. F., Bayer, B. C., Blume, R., Worsley, M. A., MoberlyChan, W. J., Shaw, E. L. ., Schlogl, R., Hart, A. J., Hofmann, S. & Wardle, B. L. (2009). Nanoscale Zirconia as a Nonmetallic Catalyst for Graphitization of Carbon and Growth of Single- and Multiwall Carbon Nanotubes, *J. Am. Chem. Soc.* **131**: 12144–12154.

Takagi, D., Hibino, H., Suzuki, S., Kobayashi, Y. & Homma, Y. (2007). Carbon Nanotube Growth from Semiconductor Nanoparticles, *Nano Lett.* **7**: 2272–2275.

Takagi, D., Homma, Y., Hibino, H., Suzuki, S. & Kobayashi, Y. (2006). Single Walled Carbon Nanotube Growth from Highly Activated Metal Nanoparticles, *Nano Lett.* **6**: 2642–2645.

Takagi, D., Kobayashi, Y., Hibino, H., Suzuki, S. & Homma, Y. (2008). Mechanism of Gold-Catalyzed Carbon Material Growth, *Nano Lett.* **8**: 832–835.

Takikawa, H., Miyano, R., Yatsuki, M. & Sakakibara, T. (1998). Carbon Nanotubes on SiC Powder Surface Grown by a Vacuum Heating Process, *Jpn. J. Appl. Phys.*, **2**: L187.

Uchino, T., Ayre, G. N., Smith, D. C., Hutchison, J. L., de Groot, C. H. & Ashburn, P. (2009). Growth of Single-Walled Carbon Nanotubes Using Germanium Nanocrystals Formed by Implantation, *J. Electrochem. Soc.* **156**: K144–K148.

Uchino, T., Bourdakos, K. N., Ayre, G. N., de Groot, C. H., Ashburn, P. & Smith, D. C. (2008). CMOS Compatible Synthesis of Carbon Nanotubes, *Mater. Res. Soc. Symp. Proc.* **1081**: 1081–P01–09.

Uchino, T., Bourdakos, K. N., de Groot, C. H., Ashburn, P., Kiziroglou, M. E., Dilliway, G. D. & Smith, D. C. (2005a). Catalyst Free Low Temperature Direct Growth of Carbon Nanotubes, *Proceedings of 2005 5th IEEE Conference on Nanotechnology* **5**: 1–4.

Uchino, T., Bourdakos, K. N., de Groot, C. H., Ashburn, P., Kiziroglou, M. E., Dilliway, G. D. & Smith, D. C. (2005b). Metal Catalyst-Free Low-Temperature Carbon Nanotube Growth on SiGe Islands, *Appl. Phys. Lett.* **86**: 233110.

Vander Wal, R. L., Tichich, T. M. & Curtis, V. E. (2001). Substrate-support Interactions in Metal-Catalyzed Carbon Nanofiber Growth, *Carbon* **39**: 2277–2289.

Wagner, R. S. & Ellis, W. C. (1964). Vapor-Liquid-Solid Mechanism of Single Crystal Growth, *Appl. Phys. Lett.* **4**: 89–90.

Wang, W. P., Wen, H. C., Jian, S. R., Juang, J. Y., Lai, Y. S., Tsai, C. H., Wi, W. F., Chen, K. T. & Chou, C. P. (2007). The Effects of Hydrogen Plasma Pretreatment on the Formation of Vertically Aligned Carbon Nanotubes, *Appl. Surf. Sci.* **253**: 9248.

Wei, Y. Y., Eres, G., Merlukov, V. I. & Lowndes, D. H. (2001). Effect of Catalyst Film Thickness on Carbon Nanotube Growth by Selective Area Chemical Vapour Deposition, *Appl. Phys. Lett.* **78**: 1394.

Yazyev, O. V. & Pasquarello, A. (2008). Effect of Metal Elements in Catalytic Growth of Carbon Nanotubes, *Phys. Rev. Lett.* **100**: 156102.

Yoshihara, N., Ago, H. & Tsuji, M. (2008). Growth Mechanism of Carbon Nanotubes over Gold-Supported Catalysts, *Jpn. J. Appl. Phys.* **47**: 1944–1948.

Yuan, D., Ding, L., Chu, H., Feng, Y., McNicholas, T. P. & Liu, J. (2008). Horizontally Aligned Single-Walled Carbon Nanotube on Quartz from a Large Variety of Metal Catalysts, *Nano Lett.* **8**: 2576–2579.

Zhou, W., Han, Z., Wang, J., Zhang, Y., Jin, Z., Sun, Z., Zhang, Y., Yan, C. & Li, Y. (2006). Copper Catalyzing Growth of Single-Walled Carbon Nanotubes on Substrates, *Nano Lett.* **6**: 2987–2990.